DOI 10.5162/sensor2015/B6.3

Gas Density and Viscosity Measurement Using Micro-Cantilever Sensor

Anastasios Badarlis[1,2], Axel Pfau[2], Anestis Kalfas[1]
[1] Aristotle University of Thessaloniki
[2] Endress+Hauser Flowtec AG
anastasios.badarlis@flowtec.endress.com

Abstract

High sensitivity and accuracy on density and viscosity measurement, especially in low pressures, can only be achieved using MEMS based sensors. In the current investigation, micro-cantilever beam from the area of atomic force microscopy was selected for the measurement of gas density and viscosity. The excitation of the beam was based on electromagnetic force, while the out of plain motion of the cantilever beam was detected with integrated piezo-resistors. The gas density and viscosity were calculated through the measurement of the resonance frequency and the quality factor. Verification of the sensor accuracy made in pure gases and mixtures as Helium, Argon, Nitrogen, Oxygen, Carbon Dioxide and Neon in atmospheric pressure. The measurement error of density and viscosity did not exceed the 2%.

Keywords: Gas density, viscosity, micro-cantilever beam, piezo-resistive.

Introduction

Accurate measurement of the gas density and viscosity can have applications in the area of gas analyzer, gas quality measurement, process diagnostics, bio applications and other. In flow measurement application, gas density can be used for the calculation of mass flow from a volume flow measurement principle, while density and viscosity in combination with the flow velocity can be used for the calculation of Reynolds number, which is an important dimensionless number of the flow.

The use of MEMS based sensor for the determination of density and viscosity has two significant advantages, these are the high sensitivity and the fast response. MEMS sensor such as micro-cantilever beams [1], [5], [6] and quartz tuning fork [4] seems to have the highest sensitivity in gases environments.

Micro-cantilever beam is the most popular geometry for a sensor of this kind. This is reasonable as their geometry is very simple and they can be easily fabricated, while a lot of researchers have presented models which describe their behavior. One very famous analysis is that of Sader [2]. Over the last twenty years micro-cantilevers models have been further developed due to their use in the atomic force microscopy (AFM).

For the current investigation, a cantilever beam from the field of the atomic force microscopy was selected, the cantilever beam placed in gaseous environment of different gases and the frequency response of the sensor measured using a lock in amplifier. Appling the right model, for the resonance frequency and quality factor, the values of density and viscosity, can be extracted.

Methods

Sensor

For the current investigation an off-the-shelf sensor was selected (*Figure 1*). The current sensor is an atomic force microscopy cantilever beam and is fabricated by the SCL-Senso.Tech. Fabrication GmbH. The small size is vital, as this makes the sensor more sensitive. The current sensor has a length of 310 um, width of 110 um and thickness 3-5 mu, while the structural material of the sensor is Si.

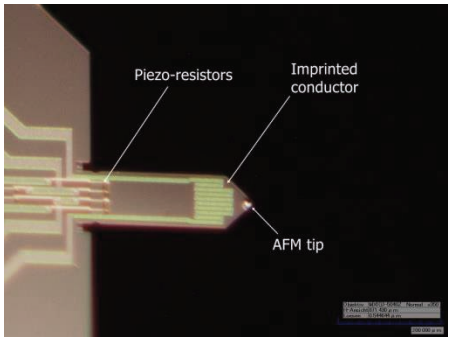

Figure 1: Atomic Force Microscopy Micro-cantilever beam.

One of the primary characteristics of the sensor is its thermal excitation with an Aluminium imprinted heater of 22 Ω. The second characteristic is its piezo-resistive sensing principle, which consists of a Wheatstone bridge with four piezo-resistors, where each has 1 kΩ. From these four piezo-resistors, two are

active and placed on the clamped side of the cantilever. A thorough characterization of a very similar sensor is presented by Fantner et al. [7]. At this point we have to make clear that, although the sensor is made to be thermal driven, the excitation principle in the current investigation is electromagnetic, as the heater was used as imprinted conductor for the generation of the Lorentz force. Using this excitation approach the excitation current stays low 1.25mA; this means that any crosstalk between the excitation wires and the piezo-resistive bridge is negligible [7].

Experimental Setup

In the following investigation six pure gases and sixteen of their binary mixtures were tested. The six gases under investigation were *He, Ar, N_2, O_2, CO_2* and *Ne*. These six gases were selected due to the large range of property variation which they have, while at the same time they are not corrosive or explosive. All of the experiments took place in atmospheric conditions (300K and 1Bar). Furthermore, the investigated gases have no or a very low percentage of humidity, below 1.5%, for this reason, the gases were considered dry.

For the experimental campaign a gas cell was built, where all of the sensors were placed. Except for the micro-cantilever beam, two reference sensors for temperature-humidity and pressure were used. During the experiments the gas cell was filled with the selected gas and the response of the sensors was recorded. The selection of gas composition into the gas cell was made by controlling the flow of two mass flow controllers. We have to mention here that except the filling gas process, during the data acquisition there was no flow and the conditions in the gas cell were considered steady.

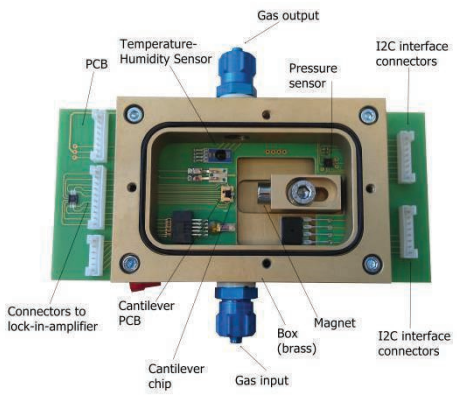

Figure 2: Gas Cell

A photo of the gas cell can be seen in *Figure 2*. It consists of a brass box, a PCB, a magnet and the sensors. All of the sensors are mounted on a PCB and through the connectors the signal passes to the electronics. Brass was selected as the material of the box, due to its high thermal conductivity. The sensor under investigation was the micro-cantilever, which was built on the cantilever chip. The magnet was placed on a slider, which makes the distance from the cantilever adjustable, which was very helpful during the mounting of the cantilever chip. Input and output connectors of the gas can also be displayed.

Sensor Modeling

The modeling of the cantilever sensor was based on the model proposed in literature [2] and [3]. In this approach, the sensor is considered as simple harmonic oscillator and the viscous and inertia effects of the gas are modeled with the help of hydrodynamic function, which can be found in the resonance frequency and in the viscous quality factor.

Measuring the resonance frequency and the quality factor of the cantilever beam and with the help of the model the density and viscosity can be extracted using an iterative algorithm.

The added mass of the fluid has an impact on the resonance frequency in the form of resonance frequency shift. This frequency shift can be calculated from Sader's analysis [2], which states that the first flexural mode ratio of the resonance to the resonance frequency in vacuum (equation (1)), has the form of equation (2) and is valid for homogeneous isotropic beams. Where Re_{Sader} is the Reynolds as is defined by Sader. In addition, *L, h, E, b,* ρ_b represent the length, the thickness, the young's modulus, the width and the density of the beam. The angular frequency of the excitation is ω, while *ρ* and *η* are the density and the viscosity of the gas. The hydrodynamic function *Γ* is derived from the solution of the linearized Navier-Stokes in the frequency domain for a cylinder beam. In case of rectangular cross-section the hydrodynamic function is adapted adding a correction, its complete form can be found in Sader's analysis [4].

$$\omega_{0,vac} = \frac{c_n^2}{L^2} h \sqrt{\frac{E}{12\rho_b}} \tag{1}$$

$$\frac{\omega_0}{\omega_{0,vac}} = \left(1 + \frac{\pi}{4} \bar{T}\, \Gamma_r (Re_{Sader})^{-0.5}\right) \tag{2}$$

$$Re_{Sader} = \rho \omega b^2 / (4\eta) \tag{3}$$

$$\bar{T} = \rho b / (\rho_b h) \tag{4}$$

The calculation of the resonance frequency for higher modes in flexural mode can be achieved

from the equation of motion for the fixed-free beam in vacuum (Bernoulli-Euler equation). In equation (1), c1 has the value of 1.8751, which is the value for the first mode and is derived solving the eigen-problem of Bernoulli-Euler equation. For the second and third mode it is has the values of 4.172 and 7.854 respectively.

Similarly, the other energy dissipation mechanisms are expressed through their quality factors. The reverse of the overall quality factor can be expressed as the sum of the partial reverse quality factors. As is presented in equation (5), three main dissipation mechanisms contribute to the overall quality factor; the viscous effect due to the surrounding fluid, the thermo-elastic dissipation and the support losses. The value of viscous fluid quality factor can be calculated from the equation (6).

$$\frac{1}{Q} = \frac{1}{Q_{Visc}} + \frac{1}{Q_{TED}} + \frac{1}{Q_{Support}} \tag{5}$$

$$Q_{Visc} = \frac{\frac{4}{\pi \bar{T}} + \Gamma_r(Re_{Sader})}{\Gamma_i(Re_{Sader})} \tag{6}$$

For pressure of 1 Bar and higher, the dominant dissipation mechanism is the fluid viscous effects. Thermo-elastic dissipation is an intrinsic structural dissipation mechanism of oscillating elements. Mathematically it can be expressed using equation (7), which is derived by Zener [8]. The quantities β_b, T_b, $c_{p,b}$ and λ_b are the thermal expansion, the temperature of the beam, the specific heat capacity and the thermal conductivity of the beam respectively.

The third source of dissipation is the support losses on the fix edge of the cantilever beam. The analytical model, which has been used in this analysis, has been developed by Hao et al. [9]. The value of the coefficient $k_{support}$ can vary and different researchers have proposed different values. In this case we consider the $k_{support}$ to be 0.34.

$$Q_{TED} = \frac{\rho_b c_{p,b}}{E\beta_b^2 T_b} \frac{1 + (\omega \frac{\rho_b c_{p,b} h^2}{\pi^2 \lambda_b})^2}{\omega \frac{\rho_b c_{p,b} h^2}{\pi^2 \lambda_b}} \tag{7}$$

$$Q_{Support} = k_{support} \frac{L^3}{h^3} \tag{8}$$

Calibration-Measurement

As in every sensor, there is discrepancy between the real behavior of the sensor and the ideal model predicted response, for this reason calibration of the sensor is needed. Calibration factors (C_1, C_2, C_3, C_4, C_5, C_6) added in equations of the model, so these equations can be rewritten. Equation (2) was replaced by the equation (9) and the convention of the Sader's Reynolds number has been adapted and has the form of equation (10). Finally, the equation for the resonance and quality factor has been extended to equations (12) and (11) respectively. Equation (12) contains a part in the parenthesis which was added to remove a systematic error and in reality is an empirical approximation.

$$\frac{\omega_0}{\omega_{0,vac}} = C_1 (1 + \frac{\pi}{C_6} \bar{T} \Gamma_r(Re_{Sader}))^{-0.5} \tag{9}$$

$$Re_{Sader} = \frac{\rho \omega b^2}{4\eta} C_2 \tag{10}$$

$$Q_{model} = Q\, C_3 + C_4 \tag{11}$$

$$f_{0,model} = \frac{\omega_0}{2\pi} (29.22((\eta - 1.9e^{-5}) + \frac{1}{500 - Q_{model}} C_5) + 1) \tag{12}$$

During the measurement process, the calculation of the gas density and viscosity for a gas is implemented by fitting the measured values of the resonance frequency ($f_{0,meas}$) and the quality factor (Q_{meas}) to the resonance and the quality factor of the model ($f_{0,model}$, Q_{model}). As can be seen the equations, the model contains the density and dynamic viscosity as parameters.

Results

Scanning the frequency in the range of 10kHz to 1MHz in air, the response of the sensor was recorded by the lock-in-amplifier. Low frequencies were not measured, due to the high noise level and the low significance for the current investigation.

In *Figure 3*, where the amplitude is presented, three flexural mode peaks are distinguishable at 34 kHz at 220 kHz and at 580 kHz. The amplitude of the first mode is one order of magnitude higher than the second, while the third mode resonance peak is two orders of magnitude lower than the first, but in reality we cannot have a direct conclusion for the real free end amplitude of each mode as they have different mode shapes. Another interesting observation in *Figure 3*, is a peak in the negative direction in the area of 180kHz. This seems to be a torsional resonance mode, which slightly influences the piezo-resistors by reducing their imposed stress.

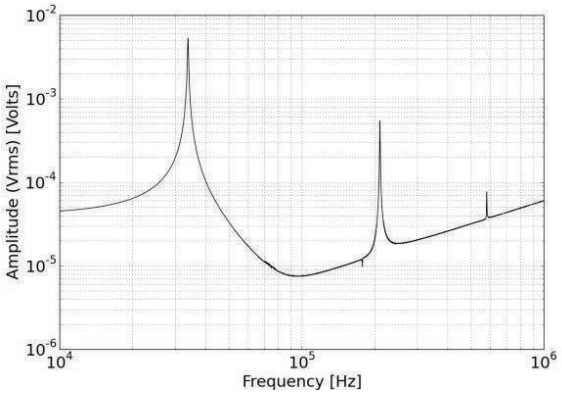

Figure 3: Amplitude spectrum of the micro-cantilever beam, response in air.

For frequencies higher than 100 kHz, the amplitude follows a linear relation with the frequency. The reason for this behavior is the inductive parasitic crosstalk effect between the piezo-restistor and the excitation conductor.

Figure 4 shows the response of the sensor in different pure gases, from a gas with very low density, in this case Helium, to a gas with high density like Argon. The bandwidth of the cantilever frequency response is 1000Hz for each gas around its resonance. In this graph, the amplitude variation and the resonance frequency shift in resonance frequency are distinguishable. The variation of response from one gas to the other is due to the variation of the density and viscosity, as was already presented in the theoretical analysis of the previous part.

The amplitude is high for the low density gases, Helium has more than the double measured voltage amplitude, or in other words deflection amplitude, than argon. Furthermore, in *Figure 4* we can observe that as the density decreases, the peak becomes sharper. The sharpness of the measurement peak is reflected in the measured quality factor.

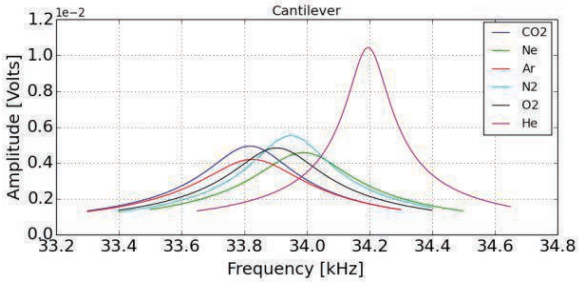

Figure 4: Measured voltage amplitude of the first flexural mode, sensitivity in resonance more than 240 Hz/(kg/m^3). Amplitude to voltage relation 20000 nm/Volt.

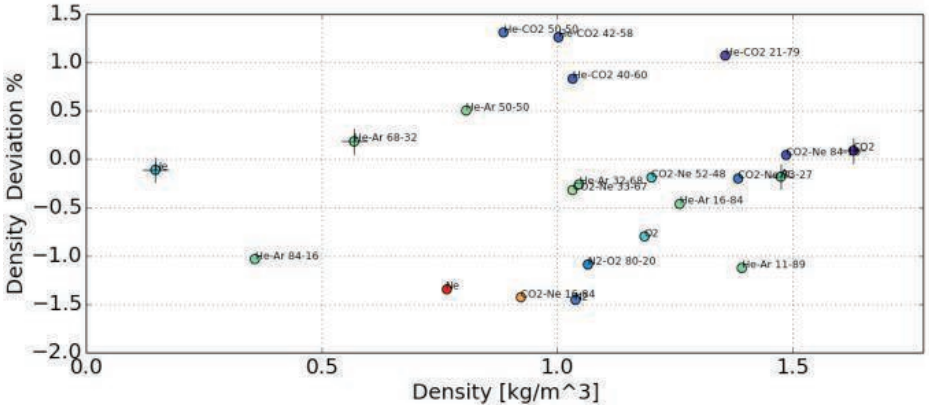

Figure 5: Deviation of measured density from the reference values.

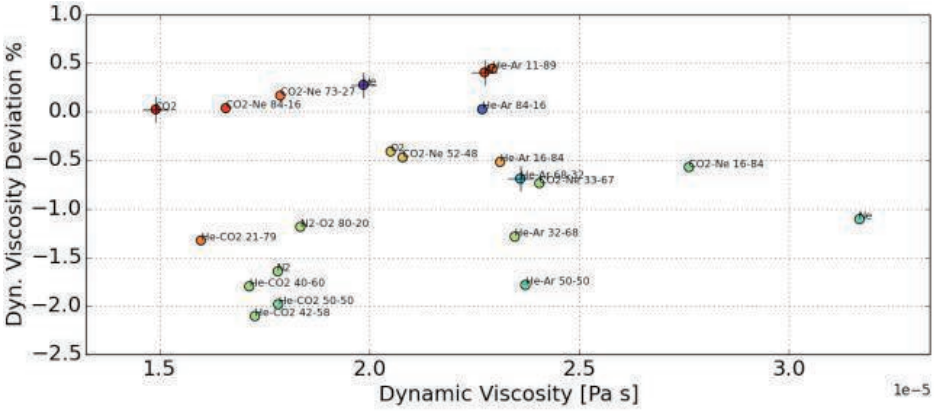

Figure 6: Deviation of measured dynamic viscosity from the reference values.

For the verification of the model and the accuracy which this can deliver, a measurement campaign with 22 gases was conducted. The test gases were selected to cover a wide range of density and viscosity in atmospheric pressure and room temperature.

As already mentioned, for the adaptation of the model, calibration is needed. Using four gases in the calibration process, the calibration coefficients were determined. The values for the specific sensor were C_1: *0.84473,* C_2: *0.4399173,* C_3: *1.1425,* C_4: *12.0811,* C_5: *0.0096839,* C_6: *4.257249*. As calibration gases was selected the He, He-Ar 68-32, Ar and CO_2. In *Figure 5* and *Figure 6* calibration gases can be indentified with one additional cross symbol.

The accuracy of the sensor, in measuring the density and dynamic viscosity, is demonstrated in *Figure 5* and *Figure 6*. The achieved accuracy of density is better than 1.5% and for dynamic viscosity is between +0.5% and -2.0%. In dynamic viscosity a systematic error seems to be present, which has the form of offset in the deviation graph.

Conclusions

Finally, in the above investigation, the performance of an AFM cantilever in measuring gas density and viscosity for a range of 22 gases has been presented. The objective of this work was to investigate the accuracy which can be achieved using as sensor, a micro-cantilever beam from AFM. The micro-cantilever beam showed very high sensitivity, which was higher than 240 Hz m^3/kg. On the other hand, the accuracy of the sensor in density is better than 1.5% and in dynamic viscosity is between +0.5% and -2.0%. The modeling of the sensor was based on Sader's analysis, where the fluid-structural interaction is mathematically described using the hydrodynamic function. Although the current investigation was conducted in atmospheric pressures, where the density of the gases is very low, the sensor was capable even of measuring accurately gases with very low density.

Acknowledgement

The authors gratefully acknowledge IST AG for providing their gas mixture facilities for our experiments and Christoph Hepp for setting it up. We would also like to thank Dr. Ernest J. Fantner and Alexander Deutschinger (SCL-Sensor.Tech.Fabrication GmbH) for providing the AFM cantilever beam. Finally, the authors would like to thank Endress+Hauser Flowtec AG for the financial support and the permission to publish the current work.

References

[1] Boskovic, S., Chon, J. W. M., Mulvaney, P., & Sader, J. E. (2002). Rheological measurements using microcantilevers. *Journal of Rheology*, *46*(4), 891.

[2] S Sader, J. E. (1998). Frequency response of cantilever beams immersed in viscous fluids with applications to the atomic force microscope. *Journal of applied physics*, *84*(1), 64-76.

[3] Van Eysden, C. a., & Sader, J. E. (2006). Resonant frequencies of a rectangular cantilever beam immersed in a fluid. *Journal of Applied Physics*, *100*(11), 114916.

[4] Sell, J. K., Niedermayer, a. O., & Jakoby, B. (2011). Simultaneous measurement of density and viscosity in gases with a quartz tuning fork resonator by tracking of the series resonance frequency. *Procedia Engineering*, *25*, 1297–1300.

[5] Goodwin, A. R. (2008). A MEMS Vibrating Edge Supported Plate for the Simultaneous Measurement of Density and Viscosity: Results for Argon, Nitrogen, and Methane at Temperatures from (297 to 373) K and Pressures between (1 and 62) MPa. *Journal of Chemical & Engineering Data*, 54(2), 536-541.

[6] Rosario, R., & Mutharasan, R. (2014). Piezoelectric excited millimeter sized cantilever sensors for measuring gas density changes. *Sensors and Actuators B: Chemical*, *192*, 99-104.

[7] Fantner, G. E., Burns, D. J., Belcher, A. M., Rangelow, I. W., & Youcef-Toumi, K. (2009). DMCMN: in depth characterization and control of AFM cantilevers with integrated sensing and actuation. *Journal of dynamic systems, measurement, and control*, 131(6), 061104.

[8] Zener, C. (1938). Internal friction in solids II. General theory of thermoelastic internal friction. *Physical Review*, 53(1), 90.

[9] Hao, Z., Erbil, A., & Ayazi, F. (2003). An analytical model for support loss in micromachined beam resonators with in-plane flexural vibrations. *Sensors and Actuators A: Physical*, 109(1), 156-164.